

Mechanisms of glacial-to-future atmospheric CO₂ effects on plant immunity

Alex Williams^{1,2}, Pierre Pétriacq^{1,2,3} , Roland E. Schwarzenbacher^{1,2}, David J. Beerling^{1,2}  and Jurriaan Ton^{1,2} 

¹Department of Animal and Plant Sciences, University of Sheffield, Sheffield, S10 2TN, UK; ²P³ Institute for Translational Soil and Plant Biology, Department of Animal and Plant Sciences, University of Sheffield, Sheffield, S10 2TN, UK; ³biOMICS Facility, Department of Animal and Plant Sciences, University of Sheffield, Sheffield, S10 2TN, UK

Summary

- The impacts of rising atmospheric CO₂ concentrations on plant disease have received increasing attention, but with little consensus emerging on the direct mechanisms by which CO₂ shapes plant immunity. Furthermore, the impact of sub-ambient CO₂ concentrations, which plants have experienced repeatedly over the past 800 000 yr, has been largely overlooked.
- A combination of gene expression analysis, phenotypic characterisation of mutants and mass spectrometry-based metabolic profiling was used to determine development-independent effects of sub-ambient CO₂ (*sa*CO₂) and elevated CO₂ (*e*CO₂) on Arabidopsis immunity.
- Resistance to the necrotrophic *Plectosphaerella cucumerina* (*Pc*) was repressed at *sa*CO₂ and enhanced at *e*CO₂. This CO₂-dependent resistance was associated with priming of jasmonic acid (JA)-dependent gene expression and required intact JA biosynthesis and signalling. Resistance to the biotrophic oomycete *Hyaloperonospora arabidopsidis* (*Hpa*) increased at both *e*CO₂ and *sa*CO₂. Although *e*CO₂ primed salicylic acid (SA)-dependent gene expression, mutations affecting SA signalling only partially suppressed *Hpa* resistance at *e*CO₂, suggesting additional mechanisms are involved. Induced production of intracellular reactive oxygen species (ROS) at *sa*CO₂ corresponded to a loss of resistance in glycolate oxidase mutants and increased transcription of the peroxisomal catalase gene *CAT2*, unveiling a mechanism by which photorespiration-derived ROS determined *Hpa* resistance at *sa*CO₂.
- By separating indirect developmental impacts from direct immunological effects, we uncover distinct mechanisms by which CO₂ shapes plant immunity and discuss their evolutionary significance.

Authors for correspondence:

Jurriaan Ton

Tel: +44 (0)114 222 0081

Email: j.ton@sheffield.ac.uk

Pierre Pétriacq

Tel: +33 (0)557 122 575

Email: pierre.petriacq@inra.fr

David J. Beerling

Tel: +44 (0)114 222 4359

Email: d.j.beerling@sheffield.ac.uk

Received: 15 July 2017

Accepted: 26 December 2017

New Phytologist (2018) 218: 752–761

doi: 10.1111/nph.15018

Key words: Arabidopsis, CO₂, defence signalling, glycolate oxidase, photorespiration, plant immunity, priming.

Introduction

Past and future changes in atmospheric CO₂ directly impact plant metabolism (Temme *et al.*, 2015), with feedbacks on resistance to pests and diseases (Strengbom & Reich, 2006; Lake & Wade, 2009; Vaughan *et al.*, 2014; Váry *et al.*, 2015; Zhang *et al.*, 2015; Mhamdi & Noctor, 2016). Although numerous effects of elevated CO₂ (*e*CO₂) on disease resistance have been reported, there is little consistency between studies. Some studies report increased disease susceptibility at *e*CO₂ (Lake & Wade, 2009; Vaughan *et al.*, 2014; Váry *et al.*, 2015), while others report no, or stimulatory, effects of *e*CO₂ on disease resistance (Strengbom & Reich, 2006; Riikonen *et al.*, 2008; Pugliese *et al.*, 2012; Zhang *et al.*, 2015; Mhamdi & Noctor, 2016). These discrepancies may arise from differences in *e*CO₂ concentrations, the duration of *e*CO₂ exposure, the method of disease quantification, species-specific adaptations to CO₂ or a combination of all these factors. Furthermore, biotrophic and necrotrophic pathogens are rarely compared within the same study, providing

limited information of how distinct components of the plant immune system respond to *e*CO₂. To date, various mechanisms by which CO₂ alters disease resistance have been proposed, ranging from changes in leaf nutrition (Strengbom & Reich, 2006), stomatal density (Lake & Wade, 2009) and pathogen-specific adaptations to altered host metabolism (Váry *et al.*, 2015). Recent evidence suggests a mechanism whereby *e*CO₂ primes pathogen-induced production of defence regulatory hormones, such as salicylic acid (SA) and jasmonic acid (JA) (Zhang *et al.*, 2015; Mhamdi & Noctor, 2016), which control defences against biotrophic and necrotrophic pathogens, respectively (Thomma *et al.*, 1998). Surprisingly, however, most studies do not take into account the stimulatory effects of CO₂ on plant development (Temme *et al.*, 2015), despite evidence that developmental stage can have a profound impact on SA-dependent and ethylene-dependent defences (Kus *et al.*, 2002; Shibata *et al.*, 2010).

Knowledge about the effects of sub-ambient CO₂ (*sa*CO₂) on plant immunity is limited and may give valuable insights into the

evolution of plant defence metabolism at typically low CO₂ (below 200 ppm) during glacial periods over the past 800 000 yr (Temme *et al.*, 2015; Galbraith & Eggleston, 2017). While stomatal processes have been implicated in defence at *sa*CO₂ (Zhou *et al.*, 2017), the contribution of *sa*CO₂ towards post-invasive plant defence remains unknown. At *sa*CO₂, net photosynthetic rate decreases as a consequence of photorespiration, along with increased stomatal conductance, increased foliar nitrogen and lower water use efficiency (Temme *et al.*, 2013; Li *et al.*, 2014). Although it remains unclear whether these changes influence disease resistance, a recent transcriptome study at *sa*CO₂ revealed enhanced activity of peroxisomal processes that correlate with changes in expression of defence-related genes (Li *et al.*, 2014). For instance, peroxisomal metabolism is stimulated at *sa*CO₂ (Li *et al.*, 2014), which can boost defence through changes in cellular redox homeostasis (Sørhagen *et al.*, 2013). The photorespiratory machinery is a major source of intracellular hydrogen peroxide (H₂O₂), which plays an important signalling role in plant defence (Chaouch *et al.*, 2010). This is further highlighted by the CATALASE-deficient *cat2* mutant, which is impaired in scavenging of peroxisomal H₂O₂ and expresses a constitutive defence phenotype (Chaouch *et al.*, 2010). Therefore, it is plausible that *sa*CO₂ influences plant resistance, but the extent, specificity and regulatory mechanisms remain unknown.

In this study, we have examined the direct impacts of *sa*CO₂ (200 ppm), *a*CO₂ (400 ppm) and *e*CO₂ (1200 ppm) on plant immunity by eliminating confounding effects of CO₂ on plant development. Using a plant development correction, we show that CO₂ has differential impacts on resistance against the biotrophic oomycete *Hyaloperonospora arabidopsidis* (*Hpa*) and the necrotrophic fungus *Plectosphaerella cucumerina* (*Pc*). Subsequent molecular and biochemical characterization of CO₂-dependent resistance phenotypes uncovered differing mechanisms by which CO₂ shapes the plant immune system. Apart from priming effects of *e*CO₂ on hormone-dependent defences, we provide evidence for a critical role of photorespiration in plant defence at *sa*CO₂ and discuss possible evolutionary implications.

Materials and Methods

Reagents and chemicals

All chemicals and reagents were purchased from Sigma-Aldrich unless stated otherwise.

Plant cultivation and growth conditions

Arabidopsis thaliana (L.) Heynh. accession Col-0 was used as wild-type plant genotype throughout this study, along with Col-0 mutant lines *npr1-1* (Cao *et al.*, 1997), *sid2-1* (Wildermuth *et al.*, 2001), *jar1-1* (Staswick, 2002), *aos1-1* (Przybyla *et al.*, 2008), *rbobD/F* (Torres *et al.*, 2002), *gox1-2* (SALK_051930; Alonso *et al.*, 2003) and *haox1-2* (SALK_022285; Alonso *et al.*, 2003). Plants were cultivated under short-day conditions (8.5 h 20°C: 15.5 h 18°C,

light : dark; 65% relative humidity). Seeds were stratified for 2 d in the dark at 4°C and planted in 60 ml pots, containing a sand : compost mixture (2 : 3). After 7 d of germination, seedlings were thinned to prevent crowding. Plants were cultivated in climate- and CO₂-controlled growth cabinets (SGC097.PPX.F; Sanyo Gallenkamp PLC, Leicester, UK) under ambient conditions (*a*CO₂; 400 ppm, i.e. µl l⁻¹), sub-ambient CO₂ (*sa*CO₂; 200 ppm) or elevated CO₂ (*e*CO₂; 1200 ppm). Growth chambers were supplemented with compressed CO₂ (BOC, Guildford, UK) or scrubbed with Sofnolime 797 (AP diving, Helston, UK) to maintain constant CO₂ at indicated concentrations.

Plant development correction

Using leaf numbers of 3- and 4.5-wk-old plants as a proxy of development stage at different CO₂ regimes (Boyes *et al.*, 2001), seed germination at *sa*CO₂ was started 7 d earlier than at *a*CO₂, whereas seed germination at *e*CO₂ was delayed by 3 d in comparison to *a*CO₂. Development correction (DC) resulted in plants with equal numbers of leaves at all three CO₂ concentrations at the day of pathogen inoculation (eight-leaf stage for *Hpa* and 18-leaf stage for *Pc*; Supporting Information Fig. S1). This experiment was repeated once with comparable results.

Pathogenicity assays

Due to its sensitivity to age-related resistance (ARR), assays with *Hpa* (strain WACO9) were conducted with relatively young plants (3 wk old at *a*CO₂, or eight-leaf stage). Plants were inoculated with 5 × 10⁴ conidiospores ml⁻¹ and left at high humidity. Shoot tissues were collected at 6 or 7 d post-inoculation (dpi) for trypan blue staining and microscopy analysis of *Hpa* colonisation, as described previously (Luna *et al.*, 2012). Briefly, levels of *Hpa* colonisation were assigned to four distinct classes, as illustrated in Fig. S2: (I) no pathogen development; (II) presence of hyphal colonisation; (III) extensive colonisation and presence of conidiophores; and (IV) extensive colonisation and the presence of conidiophores and > 10 oospores. At least 50 leaves from > 15 plants per treatment were used to determine distributions of inoculated leaves across the four *Hpa* colonization classes. Differences in class distributions between genotype–treatment combinations were analysed for statistical significance, using Fisher's exact tests (R, v.3.1.2). To ensure necrotrophic infection, assays with *Pc* (strain BMM) were based on droplet inoculation (6 µl, 5 × 10⁶ spores ml⁻¹) on four to six fully expanded leaves of eight plants at the 18-leaf stage (4.5 wk old at *a*CO₂), as described previously (Pétiacq *et al.*, 2016a). Disease progression was measured as lesion diameters at 13 dpi. Lesion diameters were averaged per plant and treated as one biological replicate. Differences in average lesion diameter per plant between treatments (*n* = 8) were analysed for statistical significance by ANOVA (R, v.3.1.2). Pathogenicity assays with the *jar1-1*, *aos1-1*, *sid2-1*, *npr1-1*, *gox1-2* and *haox1-2* mutants were repeated at least once with similar results. The results of both the *Hpa* and the *Pc* assays were verified in independent DC experiments with wild-type plants

(Col-0), using quantitative PCR (Fig. S3). Shoot material was collected at 6 dpi ($n=4$) for quantification of *Hpa* biomass; fully expanded leaves were collected at 8 dpi ($n=4$) for quantification of *Pc* biomass. The qPCR quantifications of *Hpa* and *Pc* biomass were performed with pathogen-specific primers (Table S1), using the PCR conditions described by Anderson & McDowell (2015) and Sanchez-Vallet *et al.* (2010), respectively.

Gene expression analysis by reverse-transcriptase qPCR

RNA extraction, cDNA synthesis and relative quantification of gene expression by reverse-transcriptase qPCR (RT-qPCR) were performed as described previously (Pétriacyq *et al.*, 2016a), using gene-specific primers (Table S1). Basal and hormone-induced expression of *PR1* (*AT2G14610*) and *VSP2* (*AT5G24770*) were determined in plants of the eight-leaf stage after spraying shoots with double-distilled water, 0.1 mM JA (OChemim, Olomouc, Czech Republic), or 0.5 mM SA, supplemented with 0.01% Silwet L-77 until imminent runoff. Each biological replicate in these assays consisted of four leaves from four different plants ($n=3$). Expression of *CAT2* (*AT4G35090*), *GOX1* (*AT3G14420*) and *HAOX1* (*AT3G14130*) were measured in plants of the eight-leaf stage, where each biological replicate consisted of shoot material from one plant ($n=5$). Differences in relative transcript levels were analysed for statistical significance, using Welch's *t*-test (R, v.3.1.2). RT-qPCR assays to quantify *CAT2*, *GOX1* and *HAOX1* gene expression were repeated once with similar results.

Mass spectrometry analyses

SA and JA were quantified by ultra-pressure liquid chromatography coupled to quadrupole time of flight mass spectrometry (UPLC-Q-TOF), using MS^E technology to confirm compound-specific fragmentation patterns, as detailed in Methods S1. Each biological replicate in these assays consisted of four pooled leaves from different plant ($n=5$). Untargeted metabolic profiling by UPLC-Q-TOF MS and statistical data analysis were performed as detailed in Methods S1.

In situ detection of reactive oxygen species

Extracellular reactive oxygen species (ROS) were analysed by 3,3'-diaminobenzidine (DAB) staining (Daudi & O'Brien, 2012), whereas intracellular ROS were visualised by 2',7'-dichlorofluorescein diacetate (DCFH-DA), as described previously (Pétriacyq *et al.*, 2016b). Each biological replicate in these assays consisted of one individual leaf collected from different plants ($n=10$ for DCFH-DA, $n=5$ for DAB). In both cases, mock- or *Hpa*-treated leaves were sampled at 48 h post-inoculation (hpi). ROS intensities from DAB or DCFH-DA images were obtained with an Olympus SZX12 binocular microscope (using an HQ510 1p emission filter for DCFH-DA fluorescence; excitation/emission: 492–495/517–527 nm) and quantified using Adobe PHOTOSHOP (v.CS.5), as described previously (Luna *et al.*, 2011; Pétriacyq *et al.*, 2016b).

Results

Plant development biases the assessment of CO₂-dependent disease resistance

To determine the impacts of plant development on CO₂-dependent resistance, we first characterised the growth response of Arabidopsis to CO₂ in different atmospheric CO₂ concentrations, ranging from 200 ppm (*sa*CO₂), 400 ppm (*a*CO₂) to 1200 ppm (*e*CO₂). Using the number of leaves as a marker for developmental stage (Boyes *et al.*, 2001), both 3- and 4.5-wk-old plants showed enhanced development at *e*CO₂, and reduced development at *sa*CO₂, compared to *a*CO₂ (Fig. 1a, upper panel). To determine whether these developmental effects influence disease resistance, we compared resistance phenotypes against biotrophic *Hpa* and necrotrophic *Pc* with and without correction for plant developmental stage. This DC was achieved by delaying sowing at *e*CO₂ by 3 d in comparison to plants at *a*CO₂, while starting plant cultivation at *sa*CO₂ 7 d earlier compared to plants at *a*CO₂ (Fig. S1). DC resulted in equal numbers of leaves at all CO₂ regimes at the time of pathogen inoculation (eight-leaf stage for *Hpa* and 18-leaf stage for *Pc*; Fig. 1a, lower panel). Without DC, 3-wk-old plants showed increasing levels of *Hpa* resistance at rising CO₂ concentrations (Fig. 1b, top left), whereas 4.5-wk-old plants showed enhanced *Pc* resistance at both *e*CO₂ and *sa*CO₂ (Fig. 1b, top right). This pattern of CO₂-dependent resistance phenotypes changed upon DC application. While eight-leaf plants showed enhanced *Hpa* resistance at both *sa*CO₂ and *e*CO₂ (Fig. 1b, bottom left), 18-leaf plants showed increasing levels of *Pc* resistance with rising CO₂ concentrations (Fig. 1b, bottom right). To confirm the development-independent effects of CO₂ on disease resistance, levels of *Hpa* and *Pc* colonization were quantified in an independent DC experiment, using qPCR analysis of pathogen-specific DNA (Fig. S3). The impact of DC on resistance phenotypes at *sa*CO₂ and *e*CO₂ indicates that differences in plant development bias the assessment of CO₂-dependent disease resistance against both biotrophic and necrotrophic pathogens. Accordingly, all subsequent experiments were conducted after application of DC.

Development-independent effects of *e*CO₂ on SA- and JA-dependent resistance

SA and JA play important roles in plant defence against biotrophic and necrotrophic pathogens, respectively (Thomma *et al.*, 1998). To examine the direct (development-independent) effects of *e*CO₂ on defence signalling hormones, we used UPLC coupled to tandem MS to quantify SA and JA levels. In comparison to plants at *a*CO₂, plants at *e*CO₂ showed a 69.3% and 69.4% increase in accumulation of SA and JA, respectively (Fig. 2a). While increases in hormone levels were not sufficient to induce transcription of the SA-inducible marker gene *PR1* and the JA-inducible marker gene *VSP2* directly (Fig. 2b), they were sufficient to prime augmented induction of *PR1* and *VSP2* after exogenous application of 0.5 mM SA and 0.1 mM JA, respectively (Fig. 2b). To determine the contribution of priming of SA-

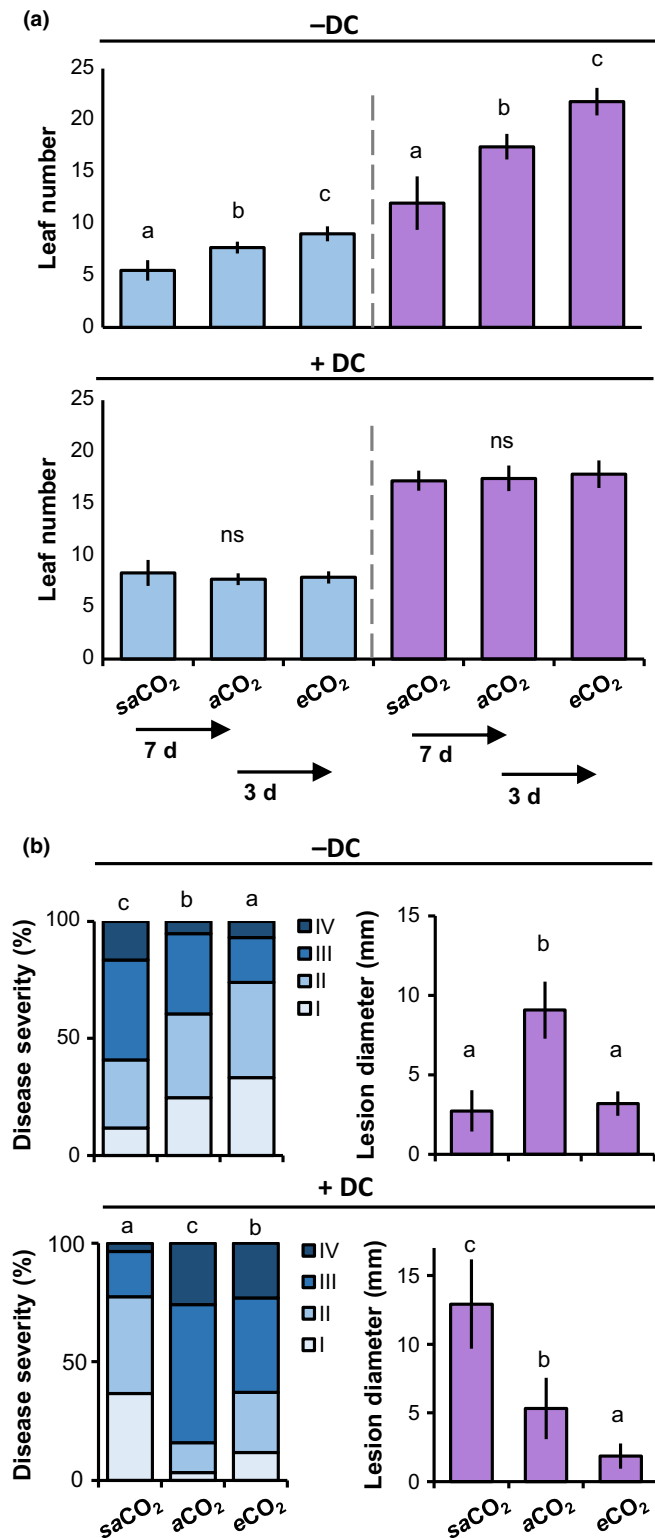


Fig. 1 Plant development correction (DC) separates immunological effects of CO₂ from indirect developmental effects on Arabidopsis resistance. (a) Effect of DC on average leaf numbers in Arabidopsis (Col-0) at sub-ambient (saCO₂; 200 ppm), ambient (aCO₂; 400 ppm) and elevated CO₂ (eCO₂; 1200 ppm). DC for saCO₂ was performed by planting seeds 7 d earlier than at aCO₂; DC for eCO₂ was achieved by planting seeds 3 d later than at aCO₂. Upper panel, leaf numbers of 3- (left) and 4.5- (right) wk-old plants without DC. Lower panel, leaf numbers after DC. Data represent mean leaf numbers (± SD, n = 10–18) and are representative of two independent experiments. ns, Not significant. (b) Effect of DC on basal resistance against biotrophic *Hyaloperonospora arabidopsidis* (*Hpa*; left) and necrotrophic *Plectosphaerella cucumerina* (*Pc*; right). Shown are relative numbers of leaves (n > 50) in *Hpa* colonization classes of increasing severity (I–IV) at 6 d post-inoculation (dpi), or average lesion diameters (± SD; n = 8) by *Pc* at 13 dpi. Different letters indicate statistically significant differences (Fisher’s exact test; ANOVA with Tukey honest significant difference post-hoc analysis; P < 0.05). Pathogenicity assays with Col-0 were repeated several times with comparable outcomes.

dependent defence is not solely responsible for eCO₂-induced resistance against *Hpa*. To determine the contribution of priming of JA-dependent defence to eCO₂-induced resistance against *Pc*, we analysed resistance phenotypes of mutants in JA production (*aos1-1*) or sensitivity (*jar1-1*). In contrast to Col-0, both *aos1-1* and *jar1-1* failed to express elevated *Pc* resistance at eCO₂ (Fig. 2d), indicating that priming of JA-inducible defence is critically important for eCO₂-induced resistance against *Pc*.

Development-independent resistance at saCO₂ relies on photorespiration-derived ROS

Basal resistance against *Hpa* was enhanced at both eCO₂ and saCO₂ (Fig. 1c). This nonlinear relationship between CO₂ and *Hpa* resistance suggests involvement of different defence mechanisms at eCO₂ and saCO₂. Unlike eCO₂ (Fig. 2b), saCO₂ did not alter basal and SA-induced *PR1* gene expression (Fig. S4a). Moreover, despite the enhanced disease susceptibility of the SA signalling mutants *sid2-1* and *npr1-1* in comparison to wild-type plants, both mutants displayed a statistically significant increase in *Hpa* resistance at saCO₂ in comparison to the same mutant background at aCO₂ (Fig. S4b). Hence, the SA-dependent defence pathway does not have a critical contribution to saCO₂-induced resistance against *Hpa*. To search for alternative mechanisms, we performed untargeted metabolite profiling of mock- and *Hpa*-inoculated plants at 24 and 72 hpi, using UPLC-Q-TOF MS (Pétiacq *et al.*, 2016b). Unsupervised principal component analysis displayed global metabolic responses, which were affected by both *Hpa* and CO₂ concentration (Fig. S5). To identify ion markers of saCO₂-induced resistance, we applied a stringent pipeline (detailed in Methods S1 and Fig. S6a) to select for ions that are significantly influenced by CO₂, *Hpa* or the interaction thereof (Fig. S6). Subsequent hierarchical clustering identified ion clusters that are either induced by saCO₂, or primed by saCO₂ for augmented induction after subsequent *Hpa* inoculation (Fig. 3). Putative ion marker identification by accurate m/z detection revealed enrichment of metabolites involved in cellular redox regulation (NAD metabolism, secondary antioxidant metabolites) and/or defence (glucosinolates, flavonoids,

dependent defence to eCO₂-induced resistance against *Hpa*, we analysed resistance phenotypes of Arabidopsis mutants impaired in SA production (*sid2-1*) or response (*npr1-1*). Although less pronounced than in wild-type plants (Col-0), both *sid2-1* and *npr1-1* expressed statistically significant levels of eCO₂-induced resistance against *Hpa* (Fig. 2c). Hence, priming of SA-

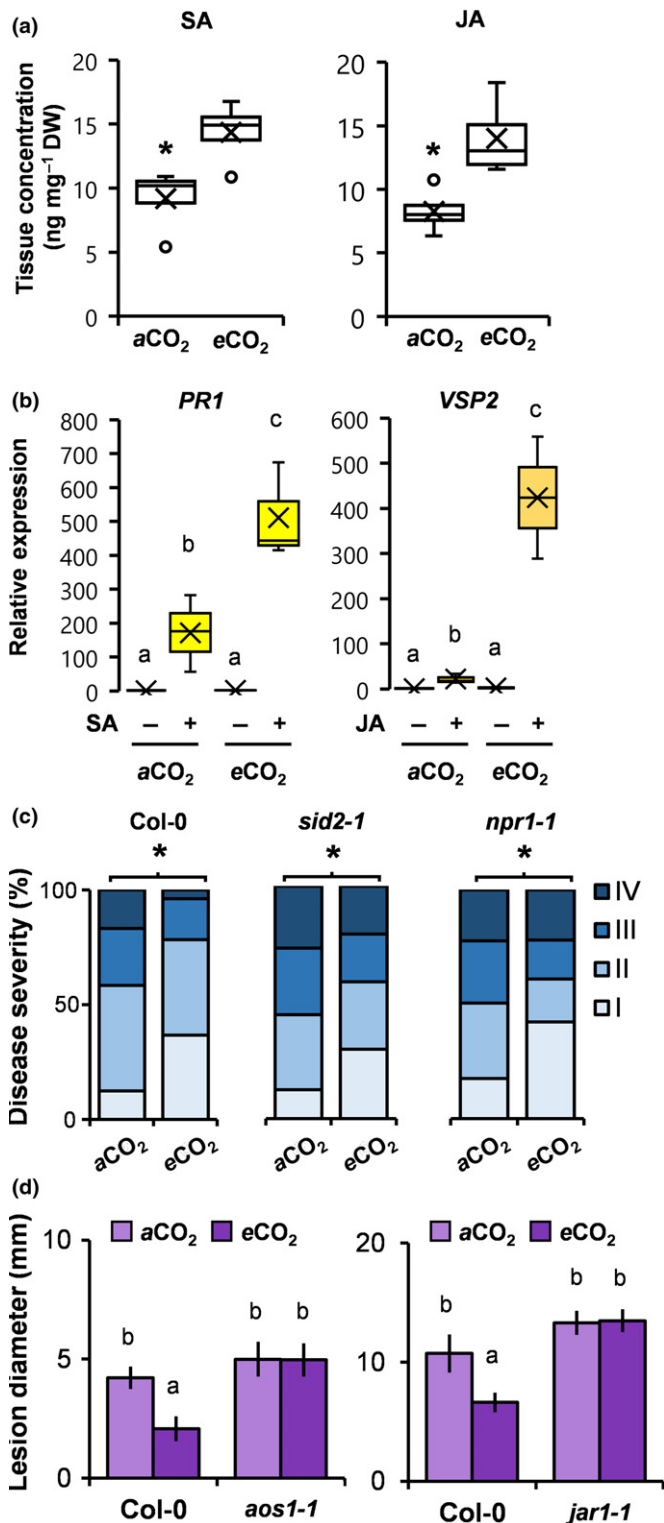


Fig. 2 Development-independent effects of elevated CO₂ (eCO₂) on salicylic acid (SA)- and jasmonic acid (JA)-dependent defence. (a) Accumulation of SA and JA acids in Arabidopsis (Col-0) of similar developmental stage (eight-leaf) at ambient CO₂ (aCO₂) (400 ppm) and eCO₂ (1200 ppm). Shown are box plots of replicated metabolite quantifications ($n = 5$; means are indicated by X; outliers outside the 2.5–97.5 percentile interval are indicated by O). (b) Responsiveness of SA- and JA-inducible genes (*PR1* and *VSP2*, respectively) in eight-leaf stage plants (Col-0) at aCO₂ and eCO₂. Shown are box plots of relative transcript levels at 8 and 24 h after treatment ($n = 3$; means are indicated by X). (c) Effects of eCO₂ on *Hyaloperonospora arabidopsidis* (*Hpa*) resistance in Col-0, the SA synthesis mutant *sid2-1* and the SA response mutant *npr1-1* at the eight-leaf stage. Shown are relative numbers of leaves ($n > 50$) in *Hpa* colonisation classes of increasing severity (I–IV) at 6 d post-inoculation (dpi). (d) Effects of eCO₂ on *Plectosphaerella cucumerina* (*Pc*) resistance in Col-0, the JA production mutant *aos1-1* and the *jar1-1* response mutant at the 18-leaf stage. Shown are average lesion diameters per plant (\pm SD; $n = 8$) of *Pc* at 13 dpi. Asterisks or different letters indicate significant differences between conditions ($P < 0.05$): (a) Welch's *t*-test; (c) Fisher's exact test; (b, d) ANOVA with Tukey honest significant difference post-hoc analysis. Pathogenicity assays with *sid2-1*, *npr1-1*, *aos1-1* and *jar1-1* were repeated once with similar results.

induced resistance. To this end, mock- and *Hpa*-inoculated leaves were stained at 48 hpi with DAB, which predominantly marks extracellular ROS production, because most DAB substrate is immediately oxidised after leaf infiltration by apoplastic H₂O₂ and peroxidases (Daudi & O'Brien, 2012). Although *Hpa*-inoculated leaves showed increased DAB staining intensity, there were no statistically significant differences in extracellular ROS intensities between *sa*CO₂ and *a*CO₂ conditions (Fig. S7a,b). Furthermore, the respiratory burst oxidase (RBOH) double mutant *rbohD/F*, which is impaired in stress-induced production of extracellular ROS (Torres *et al.*, 2002), was unaffected in *sa*CO₂-induced resistance (Fig. S7c). Hence, extracellular ROS do not play a significant role in *sa*CO₂-induced resistance. Subsequently, we stained mock- and *Hpa*-inoculated leaves with DCFH-DA, which is hydrolysed by intracellular esterases to generate DCF that reacts with intracellular ROS, yielding a fluorescent signal (Sandalo *et al.*, 2008). Although *sa*CO₂ did not increase intracellular ROS accumulation in mock-inoculated plants, *Hpa*-inoculated plants at *sa*CO₂ showed augmented ROS accumulation in comparison with *Hpa*-inoculated plants at *a*CO₂ (Fig. 4a). Thus, *sa*CO₂ primes pathogen-induced accumulation of intracellular ROS.

A major source of intracellular ROS is photorespiration, which involves production of H₂O₂ from oxidation of glycolate by glycolate oxidases (GOXs; Chaouch *et al.*, 2010; Rojas *et al.*, 2012). Loss-of-function mutations in photorespiration cause dramatic growth reduction or lethality at *a*CO₂ (Timm & Bauwe, 2013), making them unsuitable for evaluation of resistance phenotypes at *a*CO₂ and *sa*CO₂. Therefore, we selected single 'knock-down' mutants with T-DNA insertions in the promoters of *GOX* or *HAOX* (*gox1-2* and *haox1-2*, Fig. S8a), which have previously been implicated in Arabidopsis resistance (Rojas *et al.*, 2012). Despite the fact that these mutations reduced *GOX1* and *HAOX1* expression by 42.6% and 75.4%, respectively (Fig. S8b), *gox1-2* and *haox1-2* showed wild-type growth phenotypes at *sa*CO₂ (Fig. S8c). However, unlike wild-type plants (Col-0),

coumarins, alkaloids; Table S2). The cluster containing *sa*CO₂-primed markers also included traces of oxidised amino acids (Stadtman & Levine, 2003). Together, these metabolic profiles suggest that plants at *sa*CO₂ are exposed to enhanced oxidative stress due to increased production of ROS.

As ROS can act as defence signals in plants (Torres *et al.*, 2002), we next investigated a possible role for ROS in *sa*CO₂-

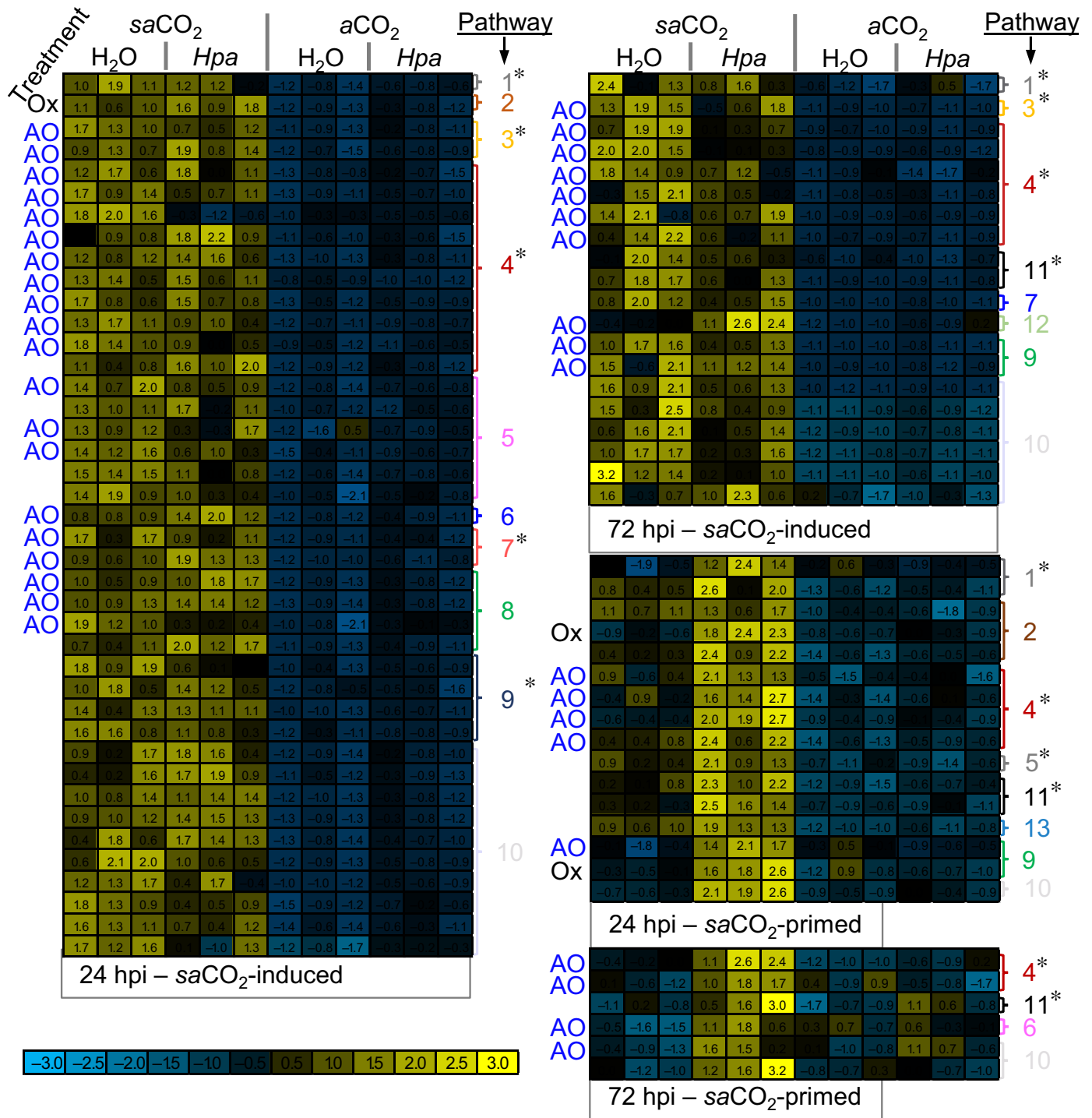


Fig. 3 Metabolic profiling of mock- and *Hyaloperonospora arabidopsidis* (*Hpa*)-inoculated *Arabidopsis* leaves of similar developmental stage at sub-ambient CO₂ (saCO₂) and ambient CO₂ (aCO₂). Plants of eight-leaf stage (Col-0) grown at saCO₂ (200 ppm) and aCO₂ (400 ppm) were mock- or *Hpa*-inoculated. Methanol extracts from leaves at 24 and 72 h post-inoculation (hpi) were analysed by UPLC-Q-TOF in negative and positive ionisation mode. Normalised ion intensities were filtered for statistically significant differences between treatments, using ANOVA ($P < 0.01$ + Benjamini–Hochberg false discovery rate correction), followed by two-way ANOVA ($P < 0.01$) to select for ion markers that are significantly influenced by CO₂, *Hpa* or the interaction thereof, at 24 and 72 hpi. Selected markers were subjected to hierarchical clustering (Pearson’s correlation). Shown are subclusters of markers showing either enhanced accumulation at saCO₂ or priming for augmented induction by *Hpa* at saCO₂. Coloured heat-maps show normalised ion intensities relative to the average and SD across all samples. Pathways corresponding to putative ion identities are shown on the right of the heat-maps; antioxidant properties of putative metabolites are indicated by ‘AO’ while putative oxidation products are indicated by ‘Ox’. Pathways with defence properties are marked with an asterisk. Pathway designations are as follows: (1) alkaloids; (2) amino acids; (3) coumarins; (4) flavonoids; (5) lipids; (6) photorespiration; (7) polyphenols; (8) redox; (9) terpenoids; (10) unknown; (11) glucosinolates; (12) polyamines; (13) phytohormones.

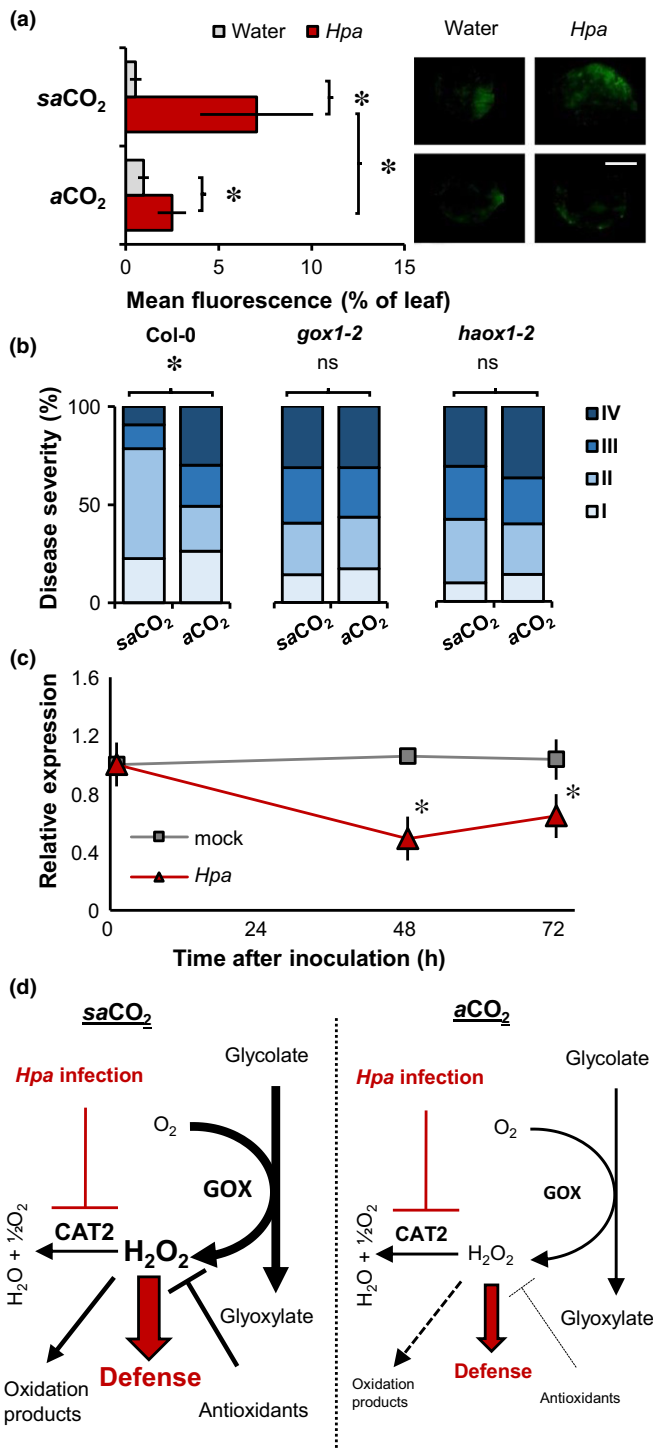


Fig. 4 Role of photorespiration in sub-ambient CO₂ (saCO₂)-induced resistance in Arabidopsis against *Hyaloperonospora arabidopsidis* (*Hpa*). (a) Quantification of intracellular H₂O₂ by 2',7'-dichlorofluorescein diacetate (DCFH-DA) staining in plants (Col-0) of similar developmental stage (eight-leaf) at saCO₂ (200 ppm) and aCO₂ (400 ppm). Shown are mean values of the fluorescent proportion of the leaf area (± SD, n = 8–10) at 48 h post-inoculation (hpi) with water mock or *Hpa*. Insets show representative staining intensities. Bar, 2 mm. (b) Quantification of *Hpa* resistance at saCO₂ and aCO₂ in wild-type plants (Col-0) and glycolate oxidase knock-down mutants *gox1-2* and *haox1-2* at the eight-leaf stage. Shown are relative numbers of leaves (n > 50) in *Hpa* colonisation classes of increasing severity (I–IV) at 7 d post-inoculation (dpi). The experiment was repeated with comparable results. (c) Impacts of *Hpa* inoculation on *CAT2* gene expression in 3-wk-old Col-0 at aCO₂ (eight-leaf stage). Shown are mean values of relative transcript abundance (± SD, n = 5) at different times after water or *Hpa* inoculation. Asterisks indicate statistically significant differences (Welch's *t*-test; Fisher's exact test; *P* < 0.05). The experiment was repeated at both saCO₂ and aCO₂, yielding comparable results (Supporting Information Fig. S9). ns, Not significant. (d) Model explaining the role of photorespiration in priming of reactive oxygen species (ROS)-dependent defence at saCO₂. Enhanced photorespiratory activity at saCO₂ causes increased production of H₂O₂ by glycolate oxidase (GOX), which is scavenged by CAT2 and antioxidant metabolites in healthy plants. *Hpa* infection represses transcription of the *CAT2* gene, causing augmented accumulation of GOX-derived H₂O₂ at saCO₂. Impacts of photorespiration on intracellular H₂O₂ are indicated by black arrows. Impacts of *Hpa* on H₂O₂-dependent defence are indicated by red arrows.

72 hpi, *Hpa*-inoculated plants showed a statistically significant reduction in *CAT2* expression (Fig. 4c), which was apparent at both saCO₂ and aCO₂ conditions (Fig. S9). Since saCO₂ boosts photorespiration (Li *et al.*, 2014), our results indicate that *Hpa*-induced *CAT2* repression triggers augmented accumulation of GOX-derived ROS during infection, which in turn results in enhanced resistance at saCO₂ (Fig. 4c).

Discussion

By eliminating bias from indirect developmental effects of CO₂ on disease resistance, we have identified distinct mechanisms by which CO₂ shapes plant immunity. There is ample evidence that plant development influences immunity through ARR (Kus *et al.*, 2002). ARR in Arabidopsis is effective against (hemi) biotrophic pathogens, including *Pseudomonas syringae* pv *tomato* (*Pst*) and *Hpa* (Kus *et al.*, 2002; McDowell *et al.*, 2005). When we conducted our experiments without DC, *Hpa* resistance intensified with increasing CO₂ concentrations (Fig. 1b). DC changed this pattern, revealing that plants of similar developmental stage expressed higher levels of *Hpa* resistance at both eCO₂ and saCO₂. These results suggest that, in the absence of DC, the resistance-enhancing effect of saCO₂ against *Hpa* is masked by low ARR of underdeveloped plants. Interestingly, DC had an opposite effect on CO₂-dependent resistance against *Pc*. Without DC, plants showed enhanced resistance at both saCO₂ and eCO₂, whereas plants of similar developmental stage (i.e. after DC) displayed increasing levels of *Pc* resistance with rising CO₂ concentrations (Fig. 1b). Thus, without DC, assessment of CO₂-dependent resistance against *Pc* is biased by defence mechanisms that are more active at earlier developmental stages.

both mutants failed to express saCO₂-induced resistance against *Hpa* (Fig. 4b), indicating a critical role for ROS-generating GOX function.

In unstressed Arabidopsis plants, GOX-derived ROS are largely scavenged by the peroxisomal catalase enzyme CAT2 (Chaouch *et al.*, 2010). To test whether the augmentation in *Hpa*-induced ROS production at saCO₂ (Fig. 4a) is related to changes in *CAT2* expression, we profiled *CAT2* transcript accumulation at different time-points after mock and *Hpa* inoculation. At both 48 and

Glucosinolates are known to accumulate to higher concentrations in younger plants (Petersen *et al.*, 2002; Brown *et al.*, 2003) and are effective against *Pc* (Frerigmann *et al.*, 2016). Alternatively, age-dependent regulation of the JA response could play a role, which is primed in younger plants due to miR156-dependent repression of JAZ6-stabilising SPL protein (Mao *et al.*, 2017). Taken together, our results show that DC is an effective method to eliminate bias from developmental effects of CO₂ on disease resistance, enabling a more accurate assessment of mechanisms by which CO₂ shapes plant immunity.

Previous studies have reported that *e*CO₂ enhances and/or primes phytohormone-dependent plant defence (Zhang *et al.*, 2015; Mhamdi & Noctor, 2016). However, none of these studies applied DC to eliminate bias from ARR. While some studies transferred plants of similar developmental age from *a*CO₂ to *e*CO₂ before pathogen inoculation (Zhang *et al.*, 2015), we opted against this method, given it can cause abrupt, and potentially confounding, changes in carbon flux. Furthermore, transferring plants from *a*CO₂ to *e*CO₂ before pathogen challenge may neglect the full extent by which *e*CO₂ affects defence hormone production (Mhamdi & Noctor, 2016). Using DC, we confirmed that *e*CO₂ enhances basal production of SA and JA (Fig. 2a), causing priming of JA- and SA-dependent gene expression, respectively (Fig. 2b). The JA signalling mutants *aos1-1* and *jar1-1* were impaired in expression of *e*CO₂-induced resistance against *Pc* (Fig. 2d), indicating a critical contribution of JA-dependent defence signalling. Conversely, the SA signalling mutants *sid2-1* and *npr1-1* were only partially affected in *e*CO₂-induced resistance against *Hpa* (Fig. 2c), indicating that priming of SA-dependent defence is not solely responsible for *Hpa* resistance at *e*CO₂, which is consistent with previous conclusions regarding *e*CO₂-induced resistance against hemi-biotrophic *Pst* (Zhang *et al.*, 2015; Mhamdi & Noctor, 2016). Furthermore, Mhamdi & Noctor (2016) recently reported that *e*CO₂-induced resistance to *Pst* is associated with changes in primary metabolism and increased pools of total and oxidised glutathione, while *Arabidopsis* mutants in glutathione regulation and NADPH-generating enzymes were affected in *Pst* resistance at *e*CO₂. Although it is unclear whether these mutants were similarly affected in basal resistance at *a*CO₂, the study by Mhamdi & Noctor (2016) concluded that oxidative pathways controlling primary metabolism played a role in *e*CO₂-induced resistance. Since carbohydrate metabolism and signalling can boost SA-dependent and SA-independent defence (Tausin & Giardina, 2014) by augmenting redox signalling (Morkunas & Ratajczak, 2014), we speculate that *e*CO₂-induced resistance in *Hpa* resistance is a consequence of changes in carbohydrate metabolism.

So far, the effects of *sa*CO₂ on plant disease resistance have received limited attention. Our DC experiments revealed that *Arabidopsis* expresses enhanced *Hpa* resistance at *sa*CO₂ (Fig. 1b). Untargeted UPLC-Q-TOF analysis revealed that this *sa*CO₂-induced resistance was associated with ion clusters displaying constitutively enhanced accumulation and/or primed accumulation after subsequent *Hpa* infection at *sa*CO₂ (Fig. 3). As these ion clusters were enriched with putative metabolites involved in redox regulation, we explored the importance of

ROS in *sa*CO₂-induced resistance. While we excluded a role for extracellular ROS (Fig. S7), plants at *sa*CO₂ showed augmented production of intracellular ROS after *Hpa* inoculation (Fig. 4a). Glycolate oxidation by GOX is a major source of intracellular H₂O₂ (Chaouch *et al.*, 2010), which probably increases at *sa*CO₂ due to enhanced photorespiration (Temme *et al.*, 2013; Li *et al.*, 2014). Moreover, GOX-derived ROS have been linked to resistance against nonhost pathogens in both *Arabidopsis* and *Nicotiana benthamiana* (Rojas *et al.*, 2012). Indeed, knockdown mutants with reduced transcription of two separate *GOX* genes failed to express enhanced *Hpa* resistance at *sa*CO₂, indicating a crucial role for photorespiratory ROS. The peroxisomal catalase enzyme, CAT2, scavenges GOX-derived H₂O₂ to mitigate oxidative damage during photorespiration (Chaouch *et al.*, 2010). Interestingly, transcriptional profiling of the *CAT2* gene revealed that *Arabidopsis* reduces *CAT2* expression after *Hpa* inoculation (Figs 4c, S9). Since *CAT2* suppresses plant defence (Polidoros *et al.*, 2001; Chaouch *et al.*, 2010), this pathogen-induced *CAT2* repression probably reflects an innate immune response to generate defence-inducing ROS during infection. In this context, we propose that stimulation of photorespiration-related GOX activity at *sa*CO₂ primes pathogen-induced accumulation of intracellular ROS. Subsequent repression of *CAT2* expression following *Hpa* attack results in enhanced accumulation of intracellular ROS, mediating enhanced levels of SA-independent resistance in comparison to *a*CO₂-exposed plants (Fig. 4d).

It is plausible that photorespiration-derived ROS were key to survival when plants adapted to glacial periods with low atmospheric CO₂. Reduced growth and plant fecundity at glacial CO₂ conditions required longer life cycles to maintain reproductive fitness (Ward & Kelly, 2004). Additionally, reduced investment in foliar defence compounds at *sa*CO₂ would have put plants at a higher risk of pathogen attack (Quirk *et al.*, 2013), creating selective pressure for a primed immune system. In addition to limiting the toxicity of 2-phosphoglycolate, we hypothesise that C₃ plants benefitted from photorespiration to prime their immune system. This hypothesis may explain why certain C₄ plants (e.g. maize) have retained photorespiration and GOX activity (Peterhansel & Maurino, 2011). Our study has uncovered a specific link between *sa*CO₂, GOX-derived ROS and enhanced immunity. This evidence supports the notion that plants have utilised photorespiratory defence signalling over glacial periods to maintain elevated levels of adaptive broad-spectrum disease resistance. This may be especially pertinent to *Arabidopsis*, which evolved under the CO₂-limited atmosphere of the Miocene epoch (Beilstein *et al.*, 2010). In this context, future initiatives to replace C₃ metabolism with C₄ metabolism in major food crops may require careful consideration of the contribution of photorespiration to plant defence.

Acknowledgements

We thank David Pardo for practical assistance. The research was supported by a consolidator grant from the European Research Council (ERC; no. 309944 'Prime-A-Plan') to J.T., a Research

Leadership Award from the Leverhulme Trust (no. RL-2012-042) to J.T., a BBSRC-IPA grant to J.T. (BB/P006698/1), and an advanced grant from ERC (no. 322998 'CDREG') to D.J.B.


Author contributions

A.W., P.P., D.J.B. and J.T. planned and conceived the experiments; A.W., R.E.S., P.P. and J.T. performed the experiments; J.T. and D.J.B. provided reagents, equipment and facilities; A.W., P.P. and J.T. analysed the data; A.W., P.P. and J.T. wrote the paper with feedback from all co-authors.

ORCID

Pierre Pétriacq  <http://orcid.org/0000-0001-8151-7420>

David J. Beerling  <https://orcid.org/0000-0003-1869-4314>

Jurriaan Ton  <https://orcid.org/0000-0002-8512-2802>

References

- Alonso JM, Stepanova AN, Leisse TJ, Kim CJ, Chen H, Shinn P, Stevenson DK, Zimmerman J, Barajas P, Cheuk R *et al.* 2003. Genome-wide insertional mutagenesis of *Arabidopsis thaliana*. *Science* **301**: 653–657.
- Anderson RG, McDowell JM. 2015. A PCR assay for the quantification of growth of the oomycete pathogen *Hyaloperonospora arabidopsidis* in *Arabidopsis thaliana*. *Molecular Plant Pathology* **16**: 893–898.
- Beilstein M, Nagalingum N, Clements M, Manchester S, Mathews S. 2010. Dated molecular phylogenies indicate a Miocene origin for *Arabidopsis thaliana*. *Proceedings of the National Academy of Sciences, USA* **107**: 18724–18728.
- Boyes DC, Zayed AM, Ascenzi R, McCaskill AJ, Hoffman NE, Davis KR, Görlach J. 2001. Growth stage-based phenotypic analysis of *Arabidopsis*: a model for high throughput functional genomics in plants. *Plant Cell* **13**: 1499–1510.
- Brown PD, Tokuhisa JG, Reichelt M, Gershenzon J. 2003. Variation of glucosinolate accumulation among different organs and developmental stages of *Arabidopsis thaliana*. *Phytochemistry* **62**: 471–481.
- Cao H, Glazebrook J, Clarke JD, Volko S, Dong X. 1997. The *Arabidopsis* NPR1 gene that controls systemic acquired resistance encodes a novel protein containing ankyrin repeats. *Cell* **88**: 57–63.
- Chaouch S, Queval G, Vanderauwera S, Mhamdi A, Vandenborgh M, Langlois-Meurinne M, Van Breusegem F, Saubert P, Noctor G. 2010. Peroxisomal hydrogen peroxide is coupled to biotic defense responses by ISOCHORISMATE SYNTHASE1 in a daylength-related manner. *Plant Physiology* **153**: 1692–1705.
- Daudi A, O'Brien JA. 2012. Detection of hydrogen peroxide by DAB staining in *Arabidopsis* leaves. *Bio-protocol* **2**: 1–5.
- Frerigmann H, Piślewska-Bednarek M, Sánchez-Vallet A, Molina A, Glawischnig E, Gigolashvili T, Bednarek P. 2016. Regulation of pathogen-triggered tryptophan metabolism in *Arabidopsis thaliana* by MYB transcription factors and indole glucosinolate conversion products. *Molecular Plant* **9**: 682–695.
- Galbraith ED, Eggleston S. 2017. A lower limit to atmospheric CO₂ concentrations over the past 800,000 years. *Nature Geoscience* **10**: 295–299.
- Kus JV, Zaton K, Sarkar R, Cameron RK. 2002. Age-related resistance in *Arabidopsis* is a developmentally regulated defense response to *Pseudomonas syringae*. *Plant Cell* **14**: 479–490.
- Lake JA, Wade RN. 2009. Plant–pathogen interactions and elevated CO₂: morphological changes in favour of pathogens. *Journal of Experimental Botany* **60**: 3123–3131.
- Li Y, Xu J, Haq NU, Zhang H, Zhu X-G. 2014. Was low CO₂ a driving force of C₄ evolution: *Arabidopsis* responses to long-term low CO₂ stress. *Journal of Experimental Botany* **65**: 3657–3667.
- Luna E, Bruce TJA, Roberts MR, Flors V, Ton J. 2012. Next-generation systemic acquired resistance. *Plant Physiology* **158**: 844–853.
- Luna E, Pastor V, Robert J, Flors V, Mauch-Mani B, Ton J. 2011. Callose deposition: a multifaceted plant defense response. *Molecular Plant–Microbe Interactions* **24**: 183–193.
- Mao Y-B, Liu Y-Q, Chen D-Y, Chen F-Y, Fang X, Hong G-J, Wang L-J, Wang J-W, Chen X-Y. 2017. Jasmonate response decay and defense metabolite accumulation contributes to age-regulated dynamics of plant insect resistance. *Nature Communications* **8**: 13925.
- McDowell JM, Williams SG, Funderburg NT, Eulgem T, Dangl JL. 2005. Genetic analysis of developmentally regulated resistance to downy mildew (*Hyaloperonospora parasitica*) in *Arabidopsis thaliana*. *Molecular Plant–Microbe Interactions* **18**: 1226–1234.
- Mhamdi A, Noctor G. 2016. High CO₂ primes plant biotic stress defences through redox-linked pathways. *Plant Physiology* **172**: 929–942.
- Morkunas I, Ratajczak L. 2014. The role of sugar signaling in plant defense responses against fungal pathogens. *Acta Physiologiae Plantarum* **36**: 1607–1619.
- Peterhansel C, Maurino VG. 2011. Photorespiration redesigned. *Plant Physiology* **155**: 49–55.
- Petersen BL, Chen S, Hansen CH, Olsen CE, Halkier BA. 2002. Composition and content of glucosinolates in developing *Arabidopsis thaliana*. *Planta* **214**: 562–571.
- Pétriacq P, Stassen J, Ton J. 2016a. Spore density determines infection strategy by the plant-pathogenic fungus *Plectosphaerella cucumerina*. *Plant Physiology* **170**: 2325–2339.
- Pétriacq P, Ton J, Patrit O, Tcherkez G, Gakière B. 2016b. NAD acts as an integral regulator of multiple defense layers. *Plant Physiology* **172**: 1465–1479.
- Polidoros AN, Mylona PV, Scandalios JG. 2001. Transgenic tobacco plants expressing the maize *Cat2* gene have altered catalase levels that affect plant–pathogen interactions and resistance to oxidative stress. *Transgenic Research* **10**: 555–569.
- Przybyla D, Göbel C, Imboden A, Hamberg M, Feussner I, Apel K. 2008. Enzymatic, but not non-enzymatic, 1O₂-mediated peroxidation of polyunsaturated fatty acids forms part of the EXECUTER1-dependent stress response program in the flu mutant of *Arabidopsis thaliana*. *Plant Journal* **54**: 236–248.
- Pugliese M, Liu J, Titone P, Garibaldi A, Gullino ML. 2012. Effects of elevated CO₂ and temperature on interactions of zucchini and powdery mildew. *Phytopathologia Mediterranea* **51**: 480–487.
- Quirk J, McDowell NG, Leake JR, Hudson PJ, Beerling DJ. 2013. Increased susceptibility to drought-induced mortality in *Sequoia sempervirens* (Cupressaceae) trees under Cenozoic atmospheric carbon dioxide starvation. *American Journal of Botany* **100**: 582–591.
- Riikonen J, Syrjälä L, Tulva I, Mänd P, Oksanen E, Poteri M, Vapaavuori E. 2008. Stomatal characteristics and infection biology of *Pyrenopeziza betulicola* in *Betula pendula* trees grown under elevated CO₂ and O₃. *Environmental Pollution* **156**: 536–543.
- Rojas CM, Senthil-Kumar M, Wang K, Ryu C-M, Kaundal A, Mysore KS. 2012. Glycolate oxidase modulates reactive oxygen species-mediated signal transduction during nonhost resistance in *Nicotiana benthamiana* and *Arabidopsis*. *Plant Cell* **24**: 336–352.
- Sánchez-Vallet A, Ramos B, Bednarek P, López G, Piślewska-Bednarek M, Schulze-Lefert P, Molina A. 2010. Tryptophan-derived secondary metabolites in *Arabidopsis thaliana* confer non-host resistance to necrotrophic *Plectosphaerella cucumerina* fungi. *Plant Journal* **63**: 115–127.
- Sandalio LM, Rodríguez-Serrano M, Romero-Puertas MC, del Río LA. 2008. Imaging of reactive oxygen species and nitric oxide *in vivo* in plant tissues. *Methods in Enzymology* **440**: 397–409.
- Shibata Y, Kawakita K, Takemoto D. 2010. Age-related resistance of *Nicotiana benthamiana* against hemibiotrophic pathogen *Phytophthora infestans* requires both ethylene- and salicylic acid-mediated signaling pathways. *Molecular Plant–Microbe Interactions* **23**: 1130–1142.
- Sørhagen K, Laxa M, Peterhansel C, Reumann S. 2013. The emerging role of photorespiration and non-photorespiratory peroxisomal metabolism in pathogen defence. *Plant Biology* **15**: 723–736.

- Stadtman ER, Levine RL. 2003. Free radical-mediated oxidation of free amino acids and amino acid residues in proteins. *Amino Acids* 25: 207–218.
- Staswick PE. 2002. Jasmonate response locus JAR1 and several related Arabidopsis genes encode enzymes of the firefly luciferase superfamily that show activity on jasmonic, salicylic, and indole-3-acetic acids in an assay for adenylation. *Plant Cell* 14: 1405–1415.
- Strengbom J, Reich PB. 2006. Elevated [CO₂] and increased N supply reduce leaf disease and related photosynthetic impacts on *Solidago rigida*. *Oecologia* 149: 519–525.
- Tauzin AS, Giardina T. 2014. Sucrose and invertases, a part of the plant defense response to the biotic stresses. *Frontiers in Plant Science* 5: art293.
- Temme AA, Cornwell WK, Cornelissen JHC, Aerts R. 2013. Meta-analysis reveals profound responses of plant traits to glacial CO₂ levels. *Ecology and Evolution* 3: 4525–4535.
- Temme AA, Liu JC, Cornwell WK, Cornelissen JHC, Aerts R. 2015. Winners always win: growth of a wide range of plant species from low to future high CO₂. *Ecology and Evolution* 5: 4949–4961.
- Thomma BP, Eggermont K, Penninckx IA, Mauch-Mani B, Vogelsang R, Cammue BP, Broekaert WF. 1998. Separate jasmonate-dependent and salicylate-dependent defense-response pathways in Arabidopsis are essential for resistance to distinct microbial pathogens. *Proceedings of the National Academy of Sciences, USA* 95: 15107–15111.
- Timm S, Bauwe H. 2013. The variety of photorespiratory phenotypes – employing the current status for future research directions on photorespiration. *Plant Biology* 15: 737–747.
- Torres MA, Dangel JL, Jones JDG. 2002. Arabidopsis gp91^{phox} homologues *AtrbohD* and *AtrbohF* are required for accumulation of reactive oxygen intermediates in the plant defense response. *Proceedings of the National Academy of Sciences, USA* 99: 517–522.
- Váry Z, Mullins E, McElwain JC, Doohan FM. 2015. The severity of wheat diseases increases when plants and pathogens are acclimatized to elevated carbon dioxide. *Global Change Biology* 21: 2661–2669.
- Vaughan MM, Huffaker A, Schmelz EA, Dafoe NJ, Christensen S, Sims J, Martins VF, Swerbilow J, Romero M, Alborn HT *et al.* 2014. Effects of elevated [CO₂] on maize defence against mycotoxigenic *Fusarium verticillioides*. *Plant, Cell & Environment* 37: 2691–2706.
- Ward JK, Kelly JK. 2004. Scaling up evolutionary responses to elevated CO₂: lessons from Arabidopsis. *Ecology Letters* 7: 427–440.
- Wildermuth MC, Dewdney J, Wu G, Ausubel FM. 2001. Isochorismate synthase is required to synthesize salicylic acid for plant defence. *Nature* 414: 562–565.
- Zhang S, Li X, Sun Z, Shao S, Hu L, Ye M, Zhou Y, Xia X, Yu J, Shi K. 2015. Antagonism between phytohormone signalling underlies the variation in disease susceptibility of tomato plants under elevated CO₂. *Journal of Experimental Botany* 66: 1951–1963.
- Zhou Y, Vroegop-Vos I, Schuurink RC, Pieterse CMJ, Van Wees SCM. 2017. Atmospheric CO₂ alters resistance of Arabidopsis to *Pseudomonas syringae* by affecting abscisic acid accumulation and stomatal responsiveness to coronatine. *Frontiers in Plant Science* 8: art700.

Supporting Information

Additional Supporting Information may be found online in the Supporting Information tab for this article:

Fig. S1 Effects of CO₂ on plant development.

Fig. S2 Images of *Hpa* colonisation classes.

Fig. S3 qPCR-based quantification of *Hpa* and *Pc* biomass.

Fig. S4 Role of SA signalling in *sa*CO₂-induced resistance against *Hpa*.

Fig. S5 Global metabolic signatures of *Hpa*-inoculated Arabidopsis at *sa*CO₂ and *a*CO₂.

Fig. S6 Selection of ions that are induced or primed for *Hpa*-induced accumulation by *sa*CO₂.

Fig. S7 Extracellular H₂O₂ in *sa*CO₂-induced resistance against *Hpa*.

Fig. S8 Selection of *gox1-2* and *haox1-2* mutants.

Fig. S9 Impacts of *Hpa* inoculation on *CAT2* gene expression at *sa*CO₂ and *a*CO₂.

Table S1 Primers used in this study

Table S2 Putative identification of metabolic markers detected by UPLC-Q-TOF

Methods S1 Supplemental materials and methods.

Please note: Wiley Blackwell are not responsible for the content or functionality of any Supporting Information supplied by the authors. Any queries (other than missing material) should be directed to the *New Phytologist* Central Office.